**Showcasing research of Dr. Lan Wang *et al*. from the Laboratory of Environmental Sciences and Technology of Prof. Chuanyi Wang, Xinjiang Technical Institute of Physics & Chemistry, Chinese Academy of Sciences, China.**

Green synthesis of shape-defined anatase TiO$_2$ nanocrystals wholly exposed with {001} and {100} facets

A novel green synthetic strategy is developed for synthesizing shape-defined anatase TiO$_2$ nanocrystals with exposed high-energy facets using clay mineral as a morphology-controlling reagent, which opens up new opportunities for preparing other metal oxide crystals with well-defined facets.

As featured in:
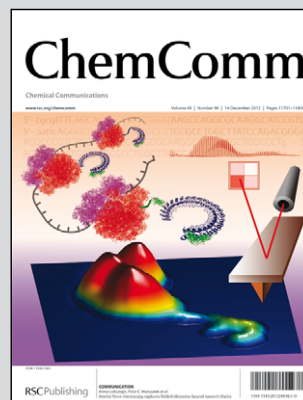
See Chuanyi Wang *et al*., *Chem. Commun.*, 2012, **48**, 11736.

RSCPublishing

www.rsc.org/chemcomm

Registered Charity Number 207890

ChemComm

COMMUNICATION

Green synthesis of shape-defined anatase TiO$_2$ nanocrystals wholly exposed with {001} and {100} facets†

Lan Wang,[a] **Ling Zang,**[b] **Jincai Zhao**[c] **and Chuanyi Wang***[a]

Anatase TiO$_2$ nanocuboids wholly exposed with high-energy {001} and {100} facets were successfully synthesized by a novel, environmentally benign synthetic strategy using acid-delaminated vermiculite (DVMT) and tetramethylammonium hydroxide as synergistic morphology-controlling reagents, where the DVMT layers act as effective hard template selectively stabilizing the {001} facets of TiO$_2$.

Titanium dioxide (TiO$_2$), as one of the most promising semiconductor materials, has become a topic of intensive study due to its important applications in a broad range of fields, such as photocatalysis, dye-sensitive solar cells, photochromic devices and gas sensing.[1–4] The performance of TiO$_2$ is not only governed by its composition, crystal structure and morphology, but also by its surface properties.[5] In particular, some physicochemical properties, such as adsorption, reactivity and selectivity *etc.*, largely depend on the exposed crystal facets.[6–10] In this scenario, there has been a recent increase in interest in engineering the morphology of TiO$_2$ with specifically exposed crystal facets.[11–14] For anatase TiO$_2$, theoretical studies indicate that the order of the average surface energies is γ {001} (0.90 J m^{-2}) > γ {100} (0.53 J m^{-2}) > γ {101} (0.44 J m^{-2}).[5,15] Generally, facets with high surface energies diminish rapidly during the crystal growth process as a result of reducing the total surface energy of crystals. Therefore, the most available anatase TiO$_2$ crystals are dominated by the thermodynamically stable {101} facets (more than 94%, according to the Wulff construction[15]), rather than the higher-energy ones such as {001} and {100}.[15–17] Yang *et al.* recently synthesized micrometre-sized anatase TiO$_2$ single crystallites with a large percentage of exposed {001} facets by using fluorine to stabilize the {001} facets.[12] Since then, tremendous efforts have been made towards the synthesis of well-defined TiO$_2$ crystals with exposed high-energy facets,[11,13,18–27] where specific

capping reagents are needed to minimize the surface energy and control the growth of TiO$_2$ crystals. Typically, F-containing species are often employed as the capping reagents to release F$^-$ ions for stabilizing the {001} facets,[9,28] which imposes serious environmental problems.[29] Therefore, it becomes increasingly desirable to develop green synthetic methodology to prepare anatase TiO$_2$ nanocrystals with exposed high-energy facets, leading to breakthroughs in the rational design of novel materials for specific practical applications.

In this work, a novel synthetic route is developed that enables the preparation of anatase TiO$_2$ nanocrystals with both {001} and {100} facets exposed; the {100} facet is relatively less studied,[8] but shows promising photoactivity as reported by Pan *et al.*[13] The synthesis represents a green approach as no fluorine-containing reagents are involved. Briefly, titanium isopropoxide (TTIP) is used as the TiO$_2$ precursor, tetramethylammonium hydroxide (Me$_4$NOH) as a dual-functional reagent, both facilitating the hydrolysis of TTIP and stabilizing the anatase polyanionic cores, [Ti$_x$O$_y$H$_{z-1}$]$^-$ formed in the early stage of crystal growth,[30] and low cost acid-delaminated vermiculite (DVMT) with surface Si–OH groups (vermiculite, a natural phyllosilicate clay mineral[31]) as the hard template controlling the morphology and growth of the crystal facets (see Fig. S1 and S2, ESI†). Combined optimization of such a reaction system leads to the formation of well-faceted anatase TiO$_2$ nanocrystals, for which the morphology and size of TiO$_2$ crystals can be controlled simply by adjusting the ratio of DVMT to TTIP in the hydrothermal reaction system (experimental details are given in the ESI†). This is the first report of using a natural clay mineral for the controlled synthesis of well shape-defined TiO$_2$ crystals with exposed high-energy facets.

Fig. 1a shows the X-ray diffraction (XRD) pattern of the TiO$_2$ crystals synthesized using a ratio of 40 g DVMT per molar TTIP (40 g mol^{-1}, corresponding to the nominal weight ratio of DVMT to TiO$_2$: 0.5), where the peaks match those of anatase TiO$_2$ (JCPDS No. 21-1272). The phase purity and chemical composition of Ti and O in the product were further confirmed by energy-dispersive X-ray spectroscopy (EDS) (Fig. S3, ESI†). A high-magnification scanning electron microscopy (SEM) image is presented in Fig. 1b, which clearly shows the well-defined morphology of tetragonal nanocuboids possessing rectangular side facets and square top/bottom facets. The selected-area electron diffraction (SAED) pattern (Fig. 1c, inset) taken from the part as marked in Fig. 1c confirms the single-crystal structure. The SAED pattern can be indexed into diffraction spots of the

[a] *Laboratory of Eco-Materials and Sustainable Technology (LEMST), Xinjiang Technical Institute of Physics & Chemistry, Chinese Academy of Sciences, Urumqi, 830011, China. E-mail: cywang@ms.xjb.ac.cn; Fax: +86-991-3838957; Tel: +86-991-3835879*
[b] *Department of Materials Science and Engineering, University of Utah, Salt Lake City, UT 84108, USA*
[c] *Key Laboratory of Photochemistry, Beijing National Laboratory for Molecular Sciences, Institute of Chemistry, Chinese Academy of Sciences, Beijing, 100190, China*
† Electronic supplementary information (ESI) available: Experimental details, additional SEM, TEM and HRTEM images, FTIR spectra, EDS spectra, and schematic illustration data. See DOI: 10.1039/c2cc36005e
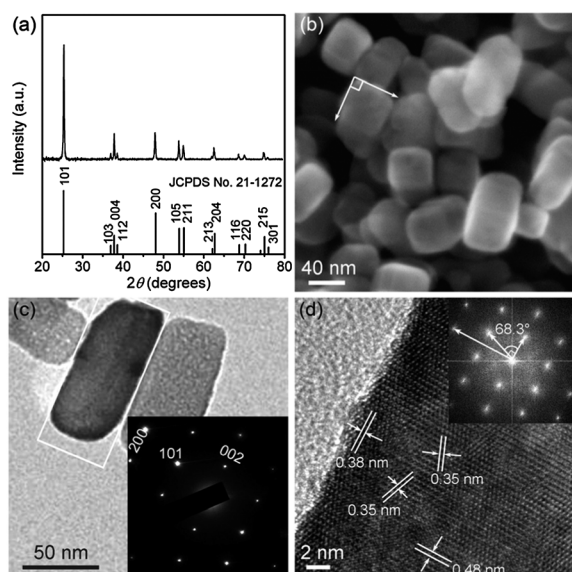
Fig. 1 (a) XRD pattern and (b) high-magnification SEM image of TiO$_2$ nanocuboids obtained in the system with a DVMT to TTIP ratio of 40 g mol^{-1}. (c) TEM image of the product, and SAED pattern recorded along the [010] orientation of a representative single crystal indicated by the rectangle (inset). (d) HRTEM image taken from the edge of the single crystal.

[010] zone axis. The high-resolution transmission electron microscopy (HRTEM) image (Fig. 1d) shows four sets of lattice fringes with spacings of 0.35, 0.35, 0.48 and 0.38 nm, which can be indexed to (101), (101), (002), and (100) planes of the anatase phase, respectively. The angles indicated in the corresponding fast-Fourier transform (FFT) image (Fig. 1d, inset) are $\sim 68.3°$ and $\sim 90°$, which are identical to the theoretical values obtained for the angles between the {101} and {001} facets and between the {100} and {001} facets, respectively.[5,12] The magnified HRTEM image (Fig. S4a, ESI†) taken from the central area of the top facet of an individual nanocuboid (bottom left inset in Fig. S4a, ESI†) shows two sets of lattices with equal spacings of 0.19 nm and an angle of 90°, which can be indexed to the (200) and (020) crystal planes. The corresponding FFT pattern (top right inset in Fig. S4a, ESI†) with sharp diffraction spots can be indexed to diffraction spots of the [001] zone.[12,23] Considering the symmetries of anatase TiO$_2$, the nanocuboids can be assigned as [001]-axis elongated single crystals with two end facets of {001} in a square shape and four side facets of {100} of rectangular shape.[25] Based on the results described above, the global morphology of a free-standing TiO$_2$ nanocuboid is schematically illustrated in Fig. S4b (ESI†), wholly exposed with two {001} and four {100} facets.

Clearly, well-faceted anatase TiO$_2$ nanocuboids with wholly exposed {001} and {100} facets were successfully synthesized in the presence of DVMT layers. In order to understand the effect of DVMT on the morphology control of anatase TiO$_2$ nano-crystals, a series of experiments were carried out by employing different amounts of DVMT. When DVMT was absent, two major types of particle morphologies, bipyramidal and rod-like, coexisting with a small amount of irregular aggregates were obtained (Fig. 2a and Fig. S5a, ESI†). HRTEM analysis indicates that the exposed facets of the bipyramidal nanocrystals are primarily {101} facets (Fig. S5b, ESI†), while the exposed
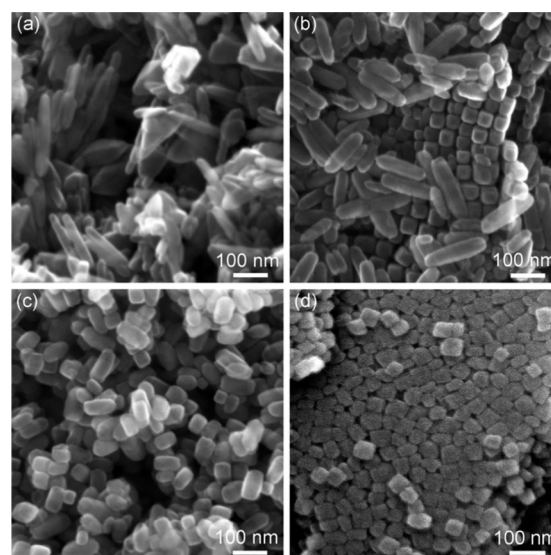

Fig. 2 SEM images of TiO$_2$ nanoparticles obtained in the system with different ratios of DVMT to TTIP: (a) 0, (b) 20, (c) 40 and (d) 80 g mol^{-1}.

facets of the rod-like nanocrystals are dominated by both {100} and {101} facets (Fig. S5c, ESI†), in agreement with what was observed previously for anatase nanocrystallites.[32–34] The formation of exposed {100} facets might be attributed to the effect of Me$_4$NOH as previously suggested.[30,35–36]

When a small amount of DVMT was added to the reaction system, elongated truncated tetragonal bipyramid nanorods (length ~ 150 nm; width ~ 35 nm) were obtained, and the morphology became more uniform (Fig. 2b and Fig. S6a, ESI†). On the basis of these observations, along with the structural analysis (Fig. S6b, ESI†) as well as the crystallographic symmetries of anatase, it is concluded that the nanorods are also single crystals with a large percentage of {100} facets at the sides and {001} facets at both ends, concurring with a small amount of {101} facets also exposed.[13,26] This indicates that the DVMT layers can stabilize the {001} facets of anatase crystals and homogeneously control the shape during growth. In other words, the solid DVMT layers likely function as shape-persistent "hard templates", helping grow the thermodynamically unfavorable crystal facets of anatase TiO$_2$. Such a templating function of DVMT layers was further verified by the formation of uniform TiO$_2$ nanocuboids with a narrower size distribution (length ~ 85 nm; edge width ~ 37 nm) as indicated by SEM analysis (Fig. 2c). When the DVMT to TTIP ratio was increased to 80 g mol^{-1}, uniform cube-like particles of anatase TiO$_2$ were obtained (Fig. 2d and Fig. S7a, ESI†), with comparable height (ca. 40 nm) and width (ca. 45 nm). The HRTEM image (Fig. S7b, ESI†) shows clear crystalline lattice fringes and the corresponding FFT pattern confirms that the particles are [001]-compressed cuboid anatase single crystals with four {100} side facets and two {001} top/bottom facets.

The above observations suggest that, with increasing DVMT content, the "hard template" effects are gradually enhanced, leading to the transformation from elongated nanorods to cube-like anatase TiO$_2$ particles (Fig. 3a), corresponding to the appearance of a larger percentage of {001} facets of anatase TiO$_2$ accompanied by the disappearance of {101} facets. Specifically, the DVMT layers can stabilize the {001} facets of anatase crystals rather than the {101} facets, which is entirely different from the

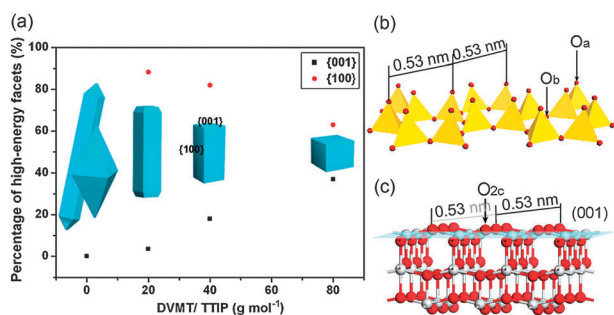**Fig. 3** (a) Relationship between the percentage of high-energy facets and the ratio of DVMT/TTIP (insets are schematic models of anatase TiO$_2$ for the different ratios of DVMT/TTIP). (b) The DVMT layer surface and O atoms represented by red spheres (O$_a$ and O$_b$ refer to apical and basal oxygen atoms, respectively). (c) (001) Surface of anatase TiO$_2$, and Ti and O atoms are represented by grey and red spheres, respectively (O$_{2c}$ refers to two fold O).

previous strategy in which F$^-$ ions interact strongly with {001} facets to reduce the surface energy leading to the preferential formation of these facets.[12,18,25,28] In the present system, the selective interaction of the DVMT layers with the {001} facets is understandable when comparing the surface structures of the (001) and (101) planes of anatase TiO$_2$. The exposed external surfaces of the DVMT layers were covered by Si–OH groups (where the O are apical oxygen atoms O$_a$ of the SiO$_4$ tetrahedral sheet), and the distance between the bridging O$_a$ atoms within the hexagonal arrangement of DVMT is 0.53 nm (Fig. 3b), which is equal to that of the bridging O$_{2c}$ atoms within the relatively flat (001) plane of TiO$_2$ (Fig. 3c). In contrast, the (101) plane of TiO$_2$ is toothed (Fig. S8, ESI†), and there are no bridging O$_{2c}$ atoms with equal distance to that of the O$_a$ atoms of the DVMT layer. In addition, the arrangement of O$_{2c}$ atoms in one (001) plane of anatase TiO$_2$ is similar to that of O$_a$ atoms of the DVMT layer (Fig. S9, ESI†). Accordingly, the hydrogen-bonding interaction of O$_{2c}$ from TiO$_2$ and H–O$_a$ from DVMT could allow the DVMT layers to selectively stabilize the {001} facets. Meanwhile, heterogeneous nucleation can occur on the surface of DVMT layers in the presence of a larger amount of DVMT, enhancing the matching of the (001) planes of anatase TiO$_2$ with the DVMT layers, thereby retarding crystal growth along the *c*-axis.

In summary, a novel and environmentally benign synthetic strategy has been developed for the synthesis of anatase TiO$_2$ nanocrystals with wholly exposed {001} and {100} facets using low cost DVMT and Me$_4$NOH as synergistic morphology-controlling reagents, and a plausible mechanism for this process is formulated on the basis of the morphological development with the ratio of DVMT to TTIP in the reaction system. Systematic investigations suggest that the DVMT layers play a critical role in selectively stabilizing the {001} facets of anatase TiO$_2$. The finding provides a facile and green approach towards the fabrication of shape-defined TiO$_2$ nanocrystals with high-energy facets preferentially exposed, and opens up new opportunities for preparing other metal oxide crystals that are of strong catalytic or photocatalytic interest. Further study into the growth mechanism of shape-defined TiO$_2$ single crystals in the presence of DVMT layers is currently ongoing in our laboratory.

Notes and references

1 X. Chen and S. S. Mao, *Chem. Rev.*, 2007, **107**, 2891.
2 A. Fujishima, X. T. Zhang and D. A. Tryk, *Surf. Sci. Rep.*, 2008, **63**, 515.
3 M. Gratzel, *Nature*, 2001, **414**, 338.
4 A. Hagfeldt, G. Boschloo, L. C. Sun, L. Kloo and H. Pettersson, *Chem. Rev.*, 2010, **110**, 6595.
5 U. Diebold, *Surf. Sci. Rep.*, 2003, **48**, 53.
6 K. Lee, M. Kim and H. Kim, *J. Mater. Chem.*, 2010, **20**, 3791.
7 Z. Y. Jiang, Q. Kuang, Z. X. Xie and L. S. Zheng, *Adv. Funct. Mater.*, 2010, **20**, 3634.
8 G. Liu, J. C. Yu, G. Q. Lu and H. M. Cheng, *Chem. Commun.*, 2011, **47**, 6763.
9 S. W. Liu, J. G. Yu and M. Jaroniec, *Chem. Mater.*, 2011, **23**, 4085.
10 Y. B. Zhao, W. H. Ma, Y. Li, H. W. Ji, C. C. Chen, H. Y. Zhu and J. C. Zhao, *Angew. Chem., Int. Ed.*, 2012, **51**, 3188.
11 Y. Q. Dai, C. M. Cobley, J. Zeng, Y. M. Sun and Y. N. Xia, *Nano Lett.*, 2009, **9**, 2455.
12 H. G. Yang, C. H. Sun, S. Z. Qiao, J. Zou, G. Liu, S. C. Smith, H. M. Cheng and G. Q. Lu, *Nature*, 2008, **453**, 638.
13 J. Pan, G. Liu, G. M. Lu and H. M. Cheng, *Angew. Chem., Int. Ed.*, 2011, **50**, 2133.
14 H. B. Jiang, Q. A. Cuan, C. Z. Wen, J. Xing, D. Wu, X. Q. Gong, C. Z. Li and H. G. Yang, *Angew. Chem., Int. Ed.*, 2011, **50**, 3764.
15 M. Lazzeri, A. Vittadini and A. Selloni, *Phys. Rev. B: Condens. Matter Mater. Phys.*, 2001, **63**, 155409.
16 M. Calatayud and C. Minot, *Surf. Sci.*, 2004, **552**, 169.
17 R. L. Penn and J. F. Banfield, *Geochim. Cosmochim. Acta*, 1999, **63**, 1549.
18 H. G. Yang, G. Liu, S. Z. Qiao, C. H. Sun, Y. G. Jin, S. C. Smith, J. Zou, H. M. Cheng and G. Q. Lu, *J. Am. Chem. Soc.*, 2009, **131**, 4078.
19 X. G. Han, Q. Kuang, M. S. Jin, Z. X. Xie and L. S. Zheng, *J. Am. Chem. Soc.*, 2009, **131**, 3152.
20 S. W. Liu, J. G. Yu and M. Jaroniec, *J. Am. Chem. Soc.*, 2010, **132**, 11914.
21 G. Liu, C. H. Sun, H. G. Yang, S. C. Smith, L. Z. Wang, G. Q. Lu and H. M. Cheng, *Chem. Commun.*, 2010, **46**, 755.
22 J. S. Chen, Y. L. Tan, C. M. Li, Y. L. Cheah, D. Y. Luan, S. Madhavi, F. Y. C. Boey, L. A. Archer and X. W. Lou, *J. Am. Chem. Soc.*, 2010, **132**, 6124.
23 J. S. Chen, J. Liu, S. Z. Qiao, R. Xu and X. W. Lou, *Chem. Commun.*, 2011, **47**, 10443.
24 T. R. Gordon, M. Cargnello, T. Paik, F. Mangolini, R. T. Weber, P. Fornasiero and C. B. Murray, *J. Am. Chem. Soc.*, 2012, **134**, 6751.
25 X. W. Zhao, W. Z. Jin, J. G. Cai, J. F. Ye, Z. H. Li, Y. R. Ma, J. L. Xie and L. M. Qi, *Adv. Funct. Mater.*, 2011, **21**, 3554.
26 C. K. Nguyen, H. G. Cha and Y. S. Kang, *Cryst. Growth Des.*, 2011, **11**, 3947.
27 L. Etgar, W. Zhang, S. Gabriel, S. G. Hickey, M. K. Nazeeruddin, A. Eychmuller, B. Liu and M. Gratzel, *Adv. Mater.*, 2012, **24**, 2202.
28 K. L. Lv, B. Cheng, J. G. Yu and G. Liu, *Phys. Chem. Chem. Phys.*, 2012, **14**, 5349.
29 C. Z. Wen, H. B. Jiang, S. Z. Qiao, H. G. Yang and G. Q. Lu, *J. Mater. Chem.*, 2011, **21**, 7052.
30 A. Chemseddine and T. Moritz, *Eur. J. Inorg. Chem.*, 1999, 235.
31 M. F. Brigatti, E. Galan and B. K. G. Theng, in *Handbook of Clay Science, Developments in Clay Science*, ed. F. Bergaya, B. K. G. Theng and G. Lagaly, Elsevier, Amsterdam, 2006, ch. 2, vol. 1, pp. 43–44.
32 S. D. Burnside, V. Shklover, C. Barbe, P. Comte, F. Arendse, K. Brooks and M. Gratzel, *Chem. Mater.*, 1998, **10**, 2419.
33 D. H. Wang, J. Liu, Q. S. Huo, Z. M. Nie, W. G. Lu, R. E. Williford and Y. B. Jiang, *J. Am. Chem. Soc.*, 2006, **128**, 13670.
34 J. M. Li and D. S. Xu, *Chem. Commun.*, 2010, **46**, 2301.
35 A. S. Barnard and L. A. Curtiss, *Nano Lett.*, 2005, **5**, 1261.
36 A. S. Barnard, P. Zapol and L. A. Curtiss, *Surf. Sci.*, 2005, **582**, 173.